# Multi-Soliton and Rogue-Wave Solutions of the Higher-Order Hirota System for an Erbium-Doped Nonlinear Fiber

Da-Wei Zuo[a,b], Yi-Tian Gao[a], Yu-Hao Sun[a], Yu-Jie Feng[a], and Long Xue[a]

[a] State Key Laboratory of Software Development Environment and Ministry-of-Education Key Laboratory of Fluid Mechanics, Beijing University of Aeronautics and Astronautics, Beijing 100191, China

[b] Department of Mathematics and Physics, Shijiazhuang Tiedao University, Shijiazhuang 050043, China

Reprint requests to Y.-T. G.; E-mail: gaoyt163@163.com

Z. Naturforsch. **69a**, 521 – 531 (2014) / DOI: 10.5560/ZNA.2014-0045
Received March 17, 2014 / revised May 11, 2014 / published online August 13, 2014

The nonlinear Schrödinger (NLS) equation appears in fluid mechanics, plasma physics, etc., while the Hirota equation, a higher-order NLS equation, has been introduced. In this paper, a higher-order Hirota system is investigated, which describes the wave propagation in an erbium-doped nonlinear fiber with higher-order dispersion. By virtue of the Darboux transformation and generalized Darboux transformation, multi-soliton solutions and higher-order rogue-wave solutions are derived, beyond the published first-order consideration. Wave propagation and interaction are analyzed: (i) Bell-shape solitons, bright- and dark-rogue waves are found; (ii) the two-soliton interaction is elastic, i. e., the amplitude and velocity of each soliton remain unchanged after the interaction; (iii) the coefficient in the system affects the direction of the soliton propagation, patterns of the soliton interaction, distance, and direction of the first-order rogue-wave propagation, as well as the range and direction of the second-order rogue-wave interaction.

*Key words:* Optical Fiber; Higher-Order Hirota System; Darboux Transformation; Multi-Soliton Solutions; Rogue-Wave Solutions.
*PACS numbers:* 47.35.Fg; 05.45.Yv; 02.30.Jr

## 1. Introduction

The nonlinear Schrödinger (NLS) equation [1 – 6], one of the nonlinear evolution equations (NLEEs) with rogue-wave solutions and soliton solutions,

$$\mathrm{i}\mu_{\varsigma}+\frac{1}{2}\mu_{\zeta\zeta}+\mu^{2}\mu^{*}=0, \tag{1}$$

where $\mathrm{i}^2=-1$, has been used for the hydrodynamic rogue-waves generated by the nonlinear energy transfer in an open ocean [7] and the broadband optical pulse propagation in nonlinear fibres [8]. $^*$ denotes the complex conjugate, while $\mu$ is the envelope of the wave field and depends on the scaled spatial variable $\varsigma$ and temporal variable $\zeta$ [8 – 12]. A rogue-wave is thought of as an isolated 'huge' wave with the amplitude claimed 'much larger' than the average wave crests around it in the ocean [13], and also seen in other fields such as the Bose–Einstein condensates, optics, and superfluids [6, 7, 13 – 15]. A soliton is a solitary wave which preserves its velocity and shape after the interaction [2], i. e., the soliton can be considered as a quasi-particle [16, 17].

However, in the practical situations, the higher-order terms that take into account the third-order dispersion, self-steepening, and other nonlinear effects have to be added to (1) [18 – 21]. Thus, with the addition of terms that are responsible for the third-order dispersion and a time-delay correction to the cubic nonlinearity introduced, in the dimensionless form, a higher-order NLS equation, also called the Hirota equation [12],

$$\mathrm{i}\mu_{\varsigma}+\frac{1}{2}\mu_{\zeta\zeta}+\mu^{2}\mu^{*}+\mathrm{i}\beta\left(\mu_{\zeta\zeta\zeta}+6\mu\mu^{*}\mu_{\zeta}\right)=0, \tag{2}$$

has appeared with the rogue-wave solutions and soliton solutions obtained [12], where the two terms in (2) that enter with a real coefficient $\beta$ are, respectively, responsible for the third-order dispersion and a time-delay correction to the cubic term.

When $\beta$ is equal to zero, (2) degenerates into (1). Besides, (2) can be considered as a combination of (1)

and the modified Korteweg–de Vries equation [12]. The modified Korteweg–de Vries equation can describe the interfacial waves in two-layer liquids with gradually varying depth, Alfvén waves in interactionless plasmas, and acoustic waves in anharmonic lattices [22].

In this paper, we will work on a higher-order Hirota system, or the deformed Hirota equations, which describes the wave propagation in an erbium-doped nonlinear fiber with higher-order dispersion [23 – 26]:

$$\mathrm{i}u_t+\frac{u_{xx}}{2}+u^2u^*+\mathrm{i}a\left(u_{xxx}+6u^*uu_x\right)=g\,, \tag{3a}$$
$$g_x=-2\mathrm{i}ub\,, \tag{3b}$$
$$b_x=\mathrm{i}(ug^*-u^*g)\,, \tag{3c}$$

where $u$ is the normalized slowly-varying amplitude of the complex field envelope, $g$ is the polarization, $b$ means the population inversion, $a$, representing the strength of the higher-order linear and nonlinear effects, is a real parameter independent of the scaled temporal variable $t$ and spatial variable $x$. The Lax Pairs, Painlevé analysis, one-soliton solution, infinite conservation laws, and bi-Hamiltonian representation for (3) have been attained [23, 24]. Special cases of (3) have been seen as well: When both $g$ and $b$ are equal to zero, (3) degenerates into (2); When both $g$ and $b$ are eliminated, (3) becomes a higher-order NLEE [23, 24]:

$$\left(u\frac{\partial^2}{\partial x^2}-u_x\frac{\partial}{\partial x}\right)\left[\mathrm{i}u_t+\mathrm{i}a(u_{xxx}+6uu^*u_x)+\frac{u_{xx}}{2}+u^2u^*\right]$$
$$+2u^2\left[\mathrm{i}(uu_t^*+u_tu^*)+\mathrm{i}a(uu_{xxx}^*+u^*u_{xxx})+6\mathrm{i}auu^*(uu_x^*\right.$$
$$\left.+u^*u_x)-\frac{1}{2}(uu_{xx}^*-u^*u_{xx})\right]=0\,. \tag{4}$$

However, to our knowledge, the rogue-wave solutions, multi-soliton solutions, Darboux transformation (DT), and generalized DT of (3) have not been obtained. Beyond the first-order consideration of [25], with the aid of symbolic computation [27 – 29], in Section 2, multi-soliton solutions and DT for (3) will be obtained. In Section 3, rogue-wave solutions and generalized DT for (3) will be attained. In Section 4, soliton and rogue-wave interaction and propagation will be discussed. Section 5 will be the conclusions.

## 2. Darboux Transformation and Soliton Solutions for (3)

In this section, we will derive both the DT and $N$-soliton solutions of (3). Lax pairs for (3) are [23, 24, 30, 31]

$$\Psi_x=U\Psi\,, \tag{5a}$$
$$\Psi_t=V\Psi\,, \tag{5b}$$

with

$$\Psi=(\psi_1,\,\psi_2)^{\mathrm{T}}\,, \tag{6a}$$
$$U=\begin{bmatrix}\mathrm{i}\lambda & \mathrm{i}u\\ \mathrm{i}u^* & -\mathrm{i}\lambda\end{bmatrix}\,, \tag{6b}$$
$$V=\begin{bmatrix}v_{11} & v_{12}\\ v_{21} & -v_{11}\end{bmatrix}\,, \tag{6c}$$
$$v_{11}=4\mathrm{i}a\lambda^3-\mathrm{i}\lambda^2+\frac{\mathrm{i}uu^*}{2}-2\mathrm{i}a\lambda uu^*$$
$$+a(uu_x^*-u^*u_x)+\frac{\mathrm{i}b}{2\lambda}\,, \tag{6d}$$
$$v_{12}=4\mathrm{i}a\lambda^2u+2a\lambda u_x-\mathrm{i}\lambda u-\mathrm{i}au_{xx}$$
$$-2\mathrm{i}au^2u^*-\frac{u_x}{2}+\frac{\mathrm{i}g}{2\lambda}\,, \tag{6e}$$
$$v_{21}=4\mathrm{i}a\lambda^2u^*-2a\lambda u_x^*-\mathrm{i}\lambda u^*+\frac{u_x^*}{2}$$
$$-\mathrm{i}au_{xx}^*-2\mathrm{i}au(u^*)^2+\frac{\mathrm{i}g^*}{2\lambda}\,, \tag{6f}$$

where $^{\mathrm{T}}$ represents the transpose of a matrix or vector, $\lambda$ is a parameter independent of $x$ and $t$, and $\psi_1$, $\psi_2$ are both functions of $x$ and $t$. The compatibility condition $U_t-V_x+UV-VU=0$ leads to (3) [23, 24].

For describing the DT of (3), by virtue of a natural number $\kappa$, we will introduce a sign $^{[\kappa]}$ on the upper right corner of a function or matrix $\Upsilon$, i. e., $\Upsilon^{[\kappa]}$, that represents a new function or matrix $\Upsilon^{[\kappa]}$ coming from $\Upsilon$ via the $\kappa$-fold operations and has the same variables as those of $\Upsilon$. Especially $\Upsilon^{[0]}=\Upsilon$.

Let $[\phi_{11}(\eta_s),\phi_{12}(\eta_s)]^{\mathrm{T}}$ $(s=1,2,\cdots,N)$ be the solutions of Lax Pairs (5) at $u$ and $\lambda=\lambda_s$, where $\lambda_s$ are all the parameters independent of $x$ and $t$, $\eta_s$ and $\phi_{1k}(\eta_s)$ $(k=1,2)$ are all the functions of $x$ and $t$. The first-step DT matrix $M^{[1]}$ has the form of [4, 6, 32 – 37]

$$M^{[1]}=\begin{bmatrix}\lambda & 0\\ 0 & \lambda\end{bmatrix}-S_1\,, \tag{7}$$

with

$$S_1 = H^{[1]}\Lambda^{[1]}(H^{[1]})^{-1}, \tag{8a}$$

$$H^{[1]} = \begin{bmatrix} \phi_{11}(\eta_1) & -[\phi_{12}(\eta_1)]^* \\ \phi_{12}(\eta_1) & [\phi_{11}(\eta_1)]^* \end{bmatrix}, \tag{8b}$$

$$\Lambda^{[1]} = \begin{bmatrix} \lambda_1 & 0 \\ 0 & \lambda_1^* \end{bmatrix}, \tag{8c}$$

where $(H^{[1]})^{-1}$ is the inverse matrix of $H^{[1]}$. Therefore, by virtue of (8), the first-order solutions of (3) can be given as

$$u^{[1]} = u + \frac{2(\lambda_1-\lambda_1^*)\phi_{11}(\eta_1)[\phi_{12}(\eta_1)]^*}{\phi_{11}(\eta_1)[\phi_{11}(\eta_1)]^* + \phi_{12}(\eta_1)[\phi_{12}(\eta_1)]^*}. \tag{9}$$

Taking the seed solution $u = 0$ and

$$\phi_{11}(\eta_1) = \mathrm{e}^{\eta_1}, \tag{10a}$$

$$\phi_{12}(\eta_1) = \mathrm{e}^{-\eta_1}, \tag{10b}$$

$$\eta_1 = \mathrm{i}\lambda_1 x + 4\mathrm{i}a\lambda_1^3 t - \mathrm{i}\lambda_1^2 t \tag{10c}$$

in (9), by virtue of (3), we can obtain the one-soliton solutions $u^{[1]}$, $g^{[1]}$, and $b^{[1]}$ as

$$u^{[1]} = \frac{2\mathrm{e}^{2\eta_1}(\lambda_1-\lambda_1^*)}{\mathrm{e}^{2(\eta_1+\eta_1^*)}+1}, \quad g^{[1]} = 0, \quad b^{[1]} = 0. \tag{11}$$

For the two-soliton solutions, we take the second-step DT matrix $M^{[2]}$ as [4, 6, 33–37]

$$M^{[2]} = \begin{bmatrix} \lambda & 0 \\ 0 & \lambda \end{bmatrix} - S_2, \tag{12}$$

where

$$S_2 = H^{[2]}\Lambda^{[2]}(H^{[2]})^{-1}, \tag{13a}$$

$$H^{[2]} = \begin{bmatrix} \phi_{21}(\eta_2) & -[\phi_{22}(\eta_2)]^* \\ \phi_{22}(\eta_2) & [\phi_{21}(\eta_2)]^* \end{bmatrix}, \tag{13b}$$

$$\Lambda^{[2]} = \begin{bmatrix} \lambda_2 & 0 \\ 0 & \lambda_2^* * \end{bmatrix}, \tag{13c}$$

$$\begin{aligned} &\left[\phi_{21}(\eta_2), \phi_{22}(\eta_2)\right]^{\mathrm{T}} = \\ &M^{[1]}|_{\lambda=\lambda_2}\left[\phi_{11}(\eta_2), \phi_{12}(\eta_2)\right]^{\mathrm{T}}, \end{aligned} \tag{13d}$$

and take $[\phi_{11}(\eta_2), \phi_{12}(\eta_2)]^{\mathrm{T}}$ as

$$\phi_{11}(\eta_2) = \mathrm{e}^{\eta_2}, \tag{14a}$$

$$\phi_{12}(\eta_2) = \mathrm{e}^{-\eta_2}, \tag{14b}$$

$$\eta_2 = \mathrm{i}\lambda_2 x + 4\mathrm{i}a\lambda_2^3 t - \mathrm{i}\lambda_2^2 t. \tag{14c}$$

Thus, by virtue of (3), the two-soliton solutions $u^{[2]}$, $g^{[2]}$, and $b^{[2]}$ can be obtained as

$$u^{[2]} = u^{[1]} + \frac{2(\lambda_2-\lambda_2^*)\phi_{21}(\eta_2)[\phi_{22}(\eta_2)]^*}{\phi_{21}(\eta_2)[\phi_{21}(\eta_2)]^* + \phi_{22}(\eta_2)[\phi_{22}(\eta_2)]^*},$$
$$g^{[2]} = 0, \quad b^{[2]} = 0. \tag{15}$$

We note that (11) and (15) are both the solutions of (1) when $a = 0$.

With such a process, the $N$-soliton solutions can be derived. We take the $N$-th step DT matrix $M^{[j]}$ $(j = 3, 4, \cdots, N)$ as [4, 6, 33–37]

$$M^{[j]} = \begin{bmatrix} \lambda & 0 \\ 0 & \lambda \end{bmatrix} - S_j, \tag{16}$$

where

$$S_j = H^{[j]}\Lambda^{[j]}(H^{[j]})^{-1}, \tag{17a}$$

$$H^{[j]} = \begin{bmatrix} \phi_{j1}(\eta_j) & -[\phi_{j2}(\eta_j)]^* * \\ \phi_{j2}(\eta_j) & [\phi_{j1}(\eta_j)]^* \end{bmatrix}, \tag{17b}$$

$$\Lambda^{[j]} = \begin{bmatrix} \lambda_j & 0 \\ 0 & \lambda_j^* \end{bmatrix}, \tag{17c}$$

$$\begin{aligned} &\left[\phi_{j1}(\eta_j), \phi_{j2}(\eta_j)\right]^{\mathrm{T}} = \\ &M^{[j-1]}|_{\lambda=\lambda_j}\left[\phi_{11}(\eta_j), \phi_{12}(\eta_j)\right]^{\mathrm{T}}, \end{aligned} \tag{17d}$$

and take $\left[\phi_{11}(\eta_j), \phi_{12}(\eta_j)\right]^{\mathrm{T}}$ as

$$\phi_{11}(\eta_j) = \mathrm{e}^{\eta_j}, \tag{18a}$$

$$\phi_{12}(\eta_j) = \mathrm{e}^{-\eta_j}, \tag{18b}$$

$$\eta_j = \mathrm{i}\lambda_j x + 4\mathrm{i}a\lambda_j^3 t - \mathrm{i}\lambda_j^2 t. \tag{18c}$$

Thus, the $N$-soliton solutions $u^{[N]}$ are

$$u^{[N]} = \sum_{j=1}^{N} \frac{2(\lambda_j-\lambda_j^*)\phi_{j1}(\eta_j)[\phi_{j2}(\eta_j)]^*}{\phi_{j1}(\eta_j)[\phi_{j1}(\eta_j)]^* + \phi_{j2}(\eta_j)[\phi_{j2}(\eta_j)]^*}. \tag{19}$$

## 3. Generalized Darboux Transformation and Rogue-Wave Solutions for (3)

In this section, the generalized DT [6, 34] will be used for the rogue-wave solutions of (3). We assume that

$$\overrightarrow{\Theta}(\zeta_1 + \delta) \tag{20}$$

is a solution for Lax Pairs (5) at $u = \widetilde{u}$ and $\lambda = \zeta_1 + \delta$, where $\overrightarrow{\Theta}$ is a vector function of $x$ and $t$, $\widetilde{u}$ is solution of (3) while $\zeta_1$ and $\delta$ are both the parameters independent of $x$ and $t$. Expanding $\overrightarrow{\Theta}$ at $\zeta_1$, we have

$$\overrightarrow{\Theta}(\zeta_1 + \delta) = \overrightarrow{\Xi}_0 + \overrightarrow{\Xi}_1\delta + \overrightarrow{\Xi}_2\delta^2 + \cdots, \tag{21}$$

where $\overrightarrow{\Xi}_\ell = \frac{1}{\ell!}\frac{\partial^\ell}{\partial\zeta^\ell}\overrightarrow{\Theta}(\zeta)|_{\zeta=\zeta_1}$ $(\ell = 0,1,2,\ldots)$ are all the vector functions of $x$ and $t$. It can be shown that $\overrightarrow{\Xi}_0$ is a solution of Lax Pairs (5) at $u=\widetilde{u}$ and $\lambda=\zeta_1$ [6].

By virtue of DT (7), the generalized DT matrix $\mathcal{M}$ for the first-step generalized DT of (3) is given as

$$\mathcal{M} = \begin{bmatrix}\lambda & 0\\ 0 & \lambda\end{bmatrix} - \begin{bmatrix}\phi_{11} & -(\phi_{12})^*\\ \phi_{12} & (\phi_{11})^*\end{bmatrix} \cdot \begin{bmatrix}\zeta_1 & 0\\ 0 & \zeta_1^*\end{bmatrix}\left(\begin{bmatrix}\phi_{11} & -(\phi_{12})^*\\ \phi_{12} & (\phi_{11})^*\end{bmatrix}\right)^{-1}, \tag{22}$$

where $(\phi_{11},\phi_{12})^{\mathrm{T}} = \overrightarrow{\Xi}_0$. Thus, the first-order solutions $\widetilde{u}^{[1]}$ for (3) are

$$\widetilde{u}^{[1]} = \widetilde{u} + \frac{2(\zeta_1-\zeta_1^*)\phi_{11}(\phi_{12})^*}{\phi_{11}(\phi_{11})^* + \phi_{12}(\phi_{12})^*}. \tag{23}$$

As the second-step generalized DT, using DT (22) for (20) and taking the limit process [6], we have

$$\lim_{\delta\to0}\frac{[\mathcal{M}|_{\lambda=\zeta_1+\delta}]\overrightarrow{\Theta}}{\delta} = \lim_{\delta\to0}\frac{[\delta+\mathcal{M}|_{\lambda=\zeta_1}]\overrightarrow{\Theta}}{\delta} = \overrightarrow{\Xi}_0 + \mathcal{M}|_{\lambda=\zeta_1}\overrightarrow{\Xi}_1 = (\phi_{21},\phi_{22})^{\mathrm{T}}. \tag{24}$$

We find a solution $(\phi_{21},\phi_{22})^{\mathrm{T}}$ for Lax Pairs (5) at $u=\widetilde{u}^{[1]}$ and $\lambda=\zeta_1$. This allows us to find the second-order solutions $\widetilde{u}^{[2]}$ of (3):

$$\widetilde{u}^{[2]} = \widetilde{u}^{[1]} + \frac{2(\zeta_1-\zeta_1^*)\phi_{21}(\phi_{22})^*}{\phi_{21}(\phi_{21})^* + \phi_{22}(\phi_{22})^*}. \tag{25}$$

If we continue such a process, the third- and fourth-step generalized DTs for (3) might be obtained.

Let us consider the rogue-wave solutions for (3). We take the plane waves as the seed solutions,

$$u = \mathrm{e}^{-\mathrm{i}t},\ g = 2\mathrm{e}^{-\mathrm{i}t},\ b = 0. \tag{26}$$

Then, the solution $\overrightarrow{\Theta}(x,t;h)$ for Lax Pairs (5) at $\lambda=\mathrm{i}h$ is

$$\overrightarrow{\Theta}(x,t;h) = \begin{bmatrix}\mathrm{i}(\alpha_1\mathrm{e}^{A} - \alpha_2\mathrm{e}^{-A})\mathrm{e}^{-\frac{\mathrm{i}t}{2}}\\ (\alpha_2\mathrm{e}^{A} - \alpha_1\mathrm{e}^{-A})\mathrm{e}^{\frac{\mathrm{i}t}{2}}\end{bmatrix}, \tag{27}$$

where

$$\alpha_1 = \frac{(h-\sqrt{h^2-1})^{1/2}}{\sqrt{h^2-1}},\quad \alpha_2 = \frac{(h+\sqrt{h^2-1})^{1/2}}{\sqrt{h^2-1}}, \tag{28a}$$

$$A = \mu(\mathrm{i}hx+wt),\ \mu = \frac{\sqrt{h^2-1}}{\mathrm{i}h},\ w = 1+h^2-2\mathrm{i}ah-4\mathrm{i}ah^3, \tag{28b}$$

and $h$ is a parameter independent of $x$ and $t$. Taking $h=1+\varepsilon^2$ and expanding the vector function $\overrightarrow{\Theta}(x,t;\varepsilon)$ at $\varepsilon=0$, we have

$$\overrightarrow{\Theta}(x,t;\varepsilon) = \overrightarrow{\Xi}_0 + \overrightarrow{\Xi}_1\varepsilon^2 + \cdots, \tag{29}$$

where $\varepsilon$ is a parameter independent of $x$ and $t$,

$$\overrightarrow{\Xi}_0 = \begin{bmatrix}(-\mathrm{i}+4t-12\mathrm{i}at+2\mathrm{i}x)\mathrm{e}^{-\frac{\mathrm{i}t}{2}}\\ (1-4\mathrm{i}t-12at+2x)\mathrm{e}^{\frac{\mathrm{i}t}{2}}\end{bmatrix}, \tag{30a}$$

$$\overrightarrow{\Xi}_1 = \begin{bmatrix}\widehat{\widehat{\theta}}_1[1]\\ \widehat{\theta}_1[1]\end{bmatrix}, \tag{30b}$$

with

$$\widehat{\widehat{\theta}}_1[1] = \Big(3-12\mathrm{i}t-228at+48t^2-288\mathrm{i}at^2-432a^2t^2 +64\mathrm{i}t^3+576at^3-1728\mathrm{i}a^2t^3-1728a^3t^3+6x+48\mathrm{i}tx +144atx-96t^2x+576\mathrm{i}at^2x+864a^2t^2x-12x^2 -48\mathrm{i}tx^2-144atx^2+8x^3\Big)\frac{\mathrm{i}}{12}\mathrm{e}^{-\frac{\mathrm{i}t}{2}},$$

$$\widehat{\theta}_1[1] = \Big(-3-12\mathrm{i}t-228at-48t^2+288\mathrm{i}at^2+432a^2t^2 +64\mathrm{i}t^3+576at^3-1728\mathrm{i}a^2t^3-1728a^3t^3+6x-48\mathrm{i}tx -144atx-96t^2x+576\mathrm{i}at^2x+864a^2t^2x+12x^2 -48\mathrm{i}tx^2-144atx^2+8x^3\Big)\frac{1}{12}\mathrm{e}^{\frac{\mathrm{i}t}{2}}.$$

By virtue of (3), (23), and (30a), we can obtain the first-order rogue-wave solutions $\widetilde{u}^{[1]}$, $\widetilde{g}^{[1]}$, and $\widetilde{b}^{[1]}$ as

$$\widetilde{u}^{[1]} = \Big[\mathrm{e}^{-\mathrm{i}t}\big(3-16(1+9a^2)t^2-4x^2+16t(\mathrm{i}+3ax)\big)\Big] \cdot\Big[1+16(1+9a^2)t^2-48atx+4x^2\Big]^{-1}, \tag{31a}$$

$$\widetilde{g}^{[1]} = \frac{\widehat{\widehat{g^{[1]}}}}{\widehat{g^{[1]}}},\quad \widetilde{b}^{[1]} = \frac{128t(6at-x)}{\big(1+16(1+9a^2)t^2-48atx+4x^2\big)^2}, \tag{31b}$$

where

$$\widehat{\widehat{g^{[1]}}} = -\Big[2\mathrm{e}^{-\mathrm{i}t}\Big(1+16\mathrm{i}t-96t^2+288a^2t^2-256\mathrm{i}t^3 -2304\mathrm{i}a^2t^3+256t^4+4608a^2t^4+20736a^4t^4-96atx$$

$$+768\mathrm{i}at^2x-1536at^3x-13824a^3t^3x+8x^2-64\mathrm{i}tx^2$$
$$+128t^2x^2+3456a^2t^2x^2-384atx^3+16x^4\Big)\Big],$$
$$\widehat{g^{[1]}}=\left(1+16t^2+144a^2t^2-48atx+4x^2\right)^2.$$

By virtue of (3), (25), and (30b), we can obtain the second-order rogue-wave solutions $\widetilde{u}^{[2]}$, $\widetilde{g}^{[2]}$, and $\widetilde{b}^{[2]}$ as

$$\widetilde{u}^{[2]}=\frac{\widehat{\widehat{u^{[2]}}}}{\widehat{u^{[2]}}}\mathrm{e}^{-\mathrm{i}t},\quad \widetilde{g}^{[2]}=\frac{\widehat{\widehat{g^{[2]}}}}{\widehat{g^{[2]}}}2\mathrm{e}^{-\mathrm{i}t},\quad \widetilde{b}^{[2]}=\frac{\widehat{\widehat{b^{[2]}}}}{\widehat{b^{[2]}}},\tag{32}$$

where $\widehat{\widehat{u^{[2]}}}$, $\widehat{u^{[2]}}$, $\widehat{\widehat{g^{[2]}}}$, $\widehat{g^{[2]}}$, $\widehat{\widehat{b^{[2]}}}$, and $\widehat{b^{[2]}}$ are all exhibited in the Appendix.

We note that the rogue-wave solutions of (3) can not degenerate into the solutions of (1), like the soliton solutions.

If we continue such a process, the third- and fourth-order rogue-wave solutions for (3) might be obtained.

## 4. Wave Interaction and Propagation

In this section, the soliton and rogue-wave interaction and propagation will be investigated. Since the functions $|g|=0$ and $b=0$ according to (11) and (15), we will mainly plot the figures for $|u|$ in Figures 1–3.

Figures 1 and 2 show that the $u$ field is a bell-shape soliton while the $g$ and $b$ fields are both equal to zero. Moreover, Figures 1 and 2 show that $a$ has an effect on the direction of soliton propagation, i. e., Figure 1a exhibits that the direction of soliton propagation is consistent with the negative $x$-axis when $a=-2$; Figure 2a shows an example of the stationary solition of (3) when $a=-1$; Figure 2b displays that the direction of the soliton propagation is consistent with the positive $x$-axis when $a=0$.

Figure 3 shows that:

(i) The $u$ field represents the two bell-shape solitons.

(ii) Coefficient $a$ has an effect on the two-soliton interaction, i. e., Figure 3a shows that the one-bell-shape soliton catches up with the other soliton when $a=1$; Figure 3b shows the two-bell-shape-soliton head-on interaction when $a=-1$; Figure 3c shows that the one-bell-shape soliton catches up with the other soliton when $a=0$.

(iii) The two-soliton interaction is elastic, i. e., the amplitude and velocity of each soliton remain unchanged after the interaction.

Figures 4 and 5 show that the coefficient $a$ has an effect on the distance of the first-order rogue-wave propagation: it is longer in Figure 5 than in Figure 4 when $a=0$ in Figure 4 and $a=\frac{1}{3}$ in Figure 5.

Figures 5 and 6 exhibit that the coefficient $a$ has an effect on the direction of the first-order rogue-wave propagation, i. e., Figure 5 shows that the direction of the first-order rogue-wave propagation is consistent with the positive $x$-axis when $a=\frac{1}{3}$; Figure 6 shows that the direction of the first-order rogue-wave propagation is consistent with the negative $x$-axis when $a=-\frac{1}{3}$. By the way, Figures 4–6 exhibit that $u$ is a bright rogue-wave and has one wave crest and two troughs, $g$ is a dark rogue-wave and has four troughs while $b$ is a bright-rogue wave and has two wave crests and two troughs.

Figures 7 and 8 display that the coefficient $a$ has an effect on the range of the second-order rouge-wave interaction: it is larger in Figure 7a than in Figure 8a, it is larger in Figure 7b than in Figure 8b, and it is larger in Figure 7c than in Figure 8c when $a=0$ in Figure 7 and $a=-\frac{1}{6}$ in Figure 8.

Figures 8 and 9 show that the coefficient $a$ has an effect on the direction of the second-order rogue-wave interaction: Figure 8 shows that it is consistent with the negative $x$-axis when $a=-\frac{1}{6}$ and Figure 9 displays that

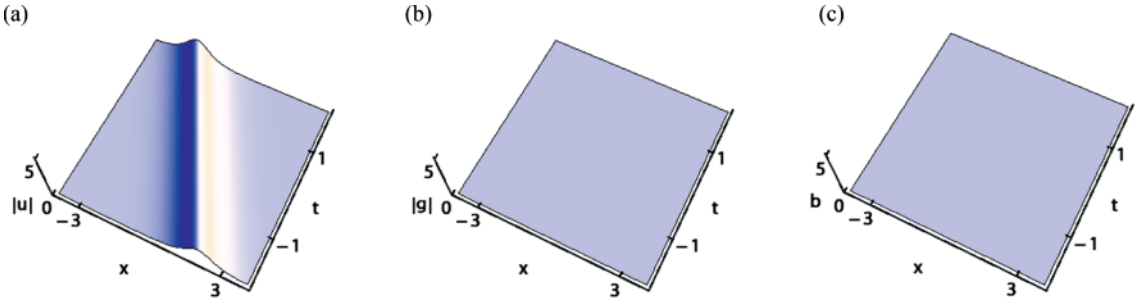


Fig. 1 (colour online). One-soliton solutions via (11) with $\lambda_1=0.5+\mathrm{i}$ and (a) of $u$ with $a=-2$; (b) of $g$; (c) of $b$.

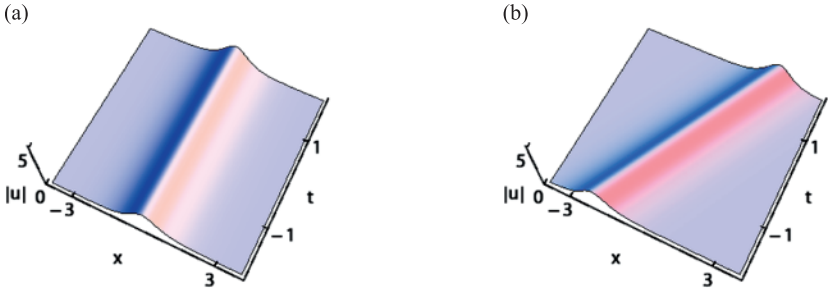


Fig. 2 (colour online). One-soliton solutions for $u$ via (11) with the parameters $\lambda_1 = 0.5 + \mathrm{i}$ and (a) of $a = -1$; (b) of $a = 0$.

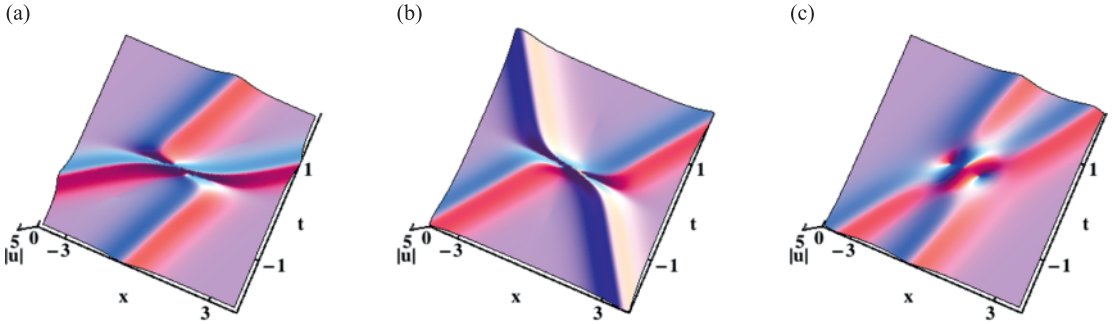


Fig. 3 (colour online). Two-soliton interaction for $u$ via (15) with $\lambda_1 = 0.6 + \mathrm{i}$, $\lambda_2 = 0.4 + \mathrm{i}$ and (a) of $a = 1$; (b) of $a = -1$; (c) of $a = 0$.

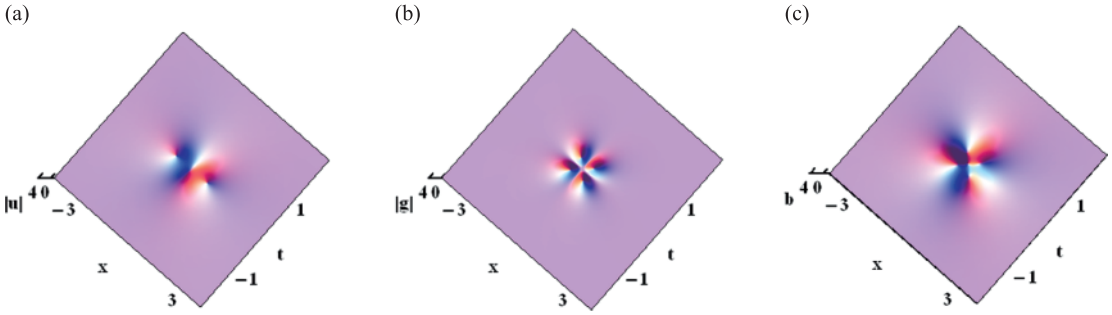


Fig. 4 (colour online). First-order rogue-wave solutions as given by (31) with $a = 0$ corresponding to (a) of $u$, (b) of $g$, and (c) of $b$.

it is consistent with the positive $x$-axis when $a = \frac{1}{3}$. By the way, Figures 7 – 9 exhibit that $u$ is a bright rogue-wave and has one wave crest and four troughs, $g$ is a dark rogue-wave and has eight troughs while $b$ is a bright rogue-wave and has four wave crests and four troughs. Figures 4 – 9 show that the dark rogue-wave $|g|$ is different from the anti-eye-shaped dark rogue-wave in [38].

## 5. Conclusions

Equation (1), the NLS equation, appears in fluid mechanics, plasma physics, etc. However, in the practical situations, the higher-order terms that take into account the third-order dispersion, self-steepening, and other nonlinear effects have to be added to (1). Thus, a higher-order NLS equation, or the Hirota equation, i. e., (2), has been introduced.

In this paper, the set of (3), a higher-order Hirota system, or a set of the deformed Hirota equations, which describes the wave propagation in an erbium-doped nonlinear fiber with higher-order dispersion, has been investigated, beyond the first-order consideration, with our results as follows:

(i) Multi-Soliton Solutions (19) and High-Order Rogue-Wave Solutions (32) for (3), generated via the DT and generalized DT, respectively, have been attained.

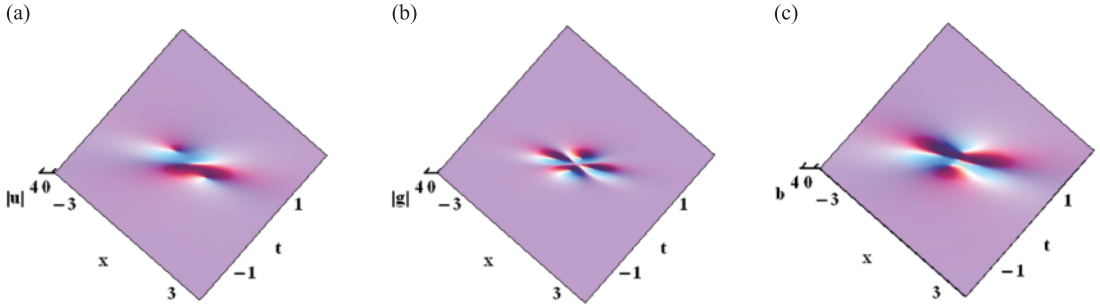


Fig. 5 (colour online). First-order rogue-wave solutions as given by (31) with $a = \frac{1}{3}$ corresponding to (a) of $u$, (b) of $g$, and (c) of $b$.

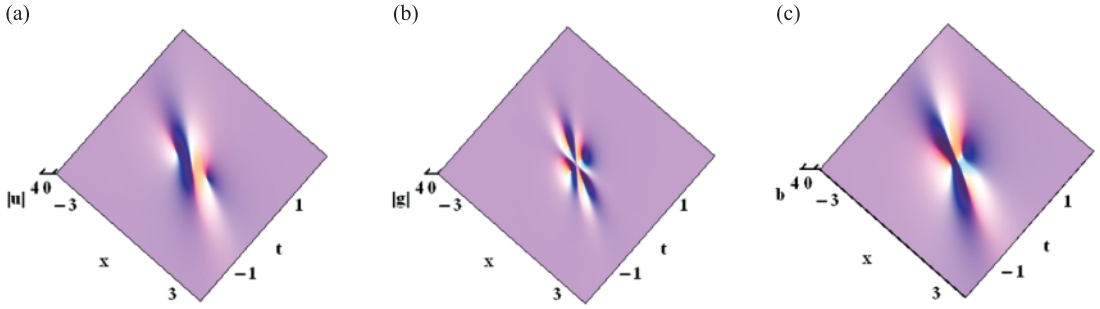


Fig. 6 (colour online). First-order rogue-wave solutions as given by (31) with $a = -\frac{1}{3}$ corresponding to (a) of $u$, (b) of $g$, and (c) of $b$.

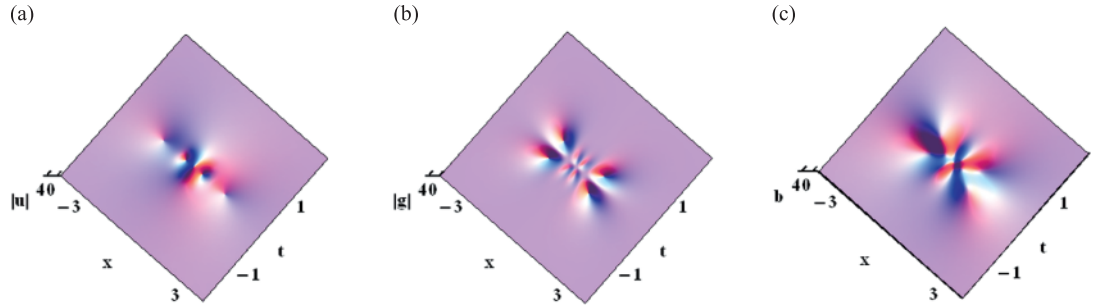


Fig. 7 (colour online). Second-order rogue-wave interaction as given by (32) with $a = 0$ corresponding to (a) of $u$, (b) of $g$, and (c) of $b$.

(ii) Solitons propagation and interaction have been analyzed:

Figures 1 and 2 have exhibited that the $u$ field is a bell-shape soliton while the $g$ and $b$ fields are both equal to zero. The coefficient $a$ has an effect on the direction of soliton propagation: Figure 1a has shown that it is consistent with the positive $x$-axis when $a = -2$; Figure 2a has displayed an example of the stationary soliton when $a = -1$; Figure 2b has exhibited that the direction of soliton propagation is consistent with the negative $x$-axis when $a = 0$.

Figure 3 has shown the interaction between the two solitons, where the $u$ field represents the two bell-shape solitons. Besides, Figure 3 has exhibited that the coefficient $a$ has an effect on the two-soliton interaction: Figure 3a has shown that the one-bell-shape soliton catches up with the other when $a = 1$; Figure 3b has exhibited the two-bell-shape soliton head-on interaction when $a = -1$; Figure 3c has shown that the one-bell-shape soliton catches up with the other when $a = 0$. Moreover, Figure 3 has displayed that the two-soliton interaction is elastic, i. e., the amplitude and velocity

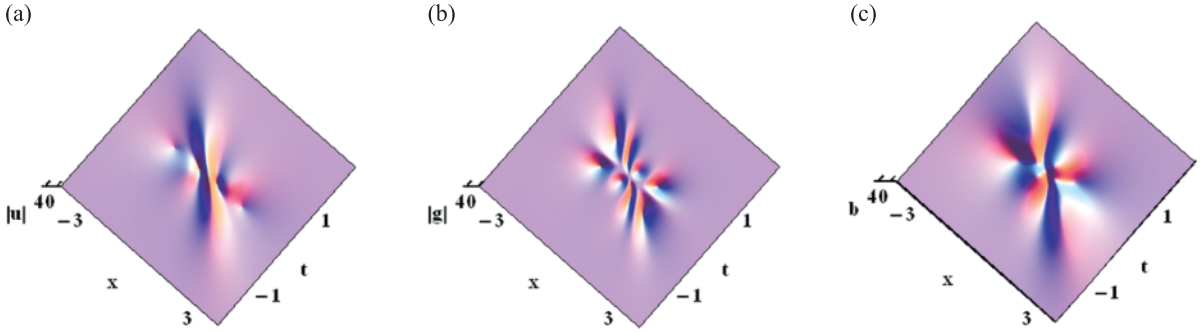


Fig. 8 (colour online). Second-order rogue-wave interaction as given by (32) with $a = -\frac{1}{6}$ corresponding to (a) of $u$, (b) of $g$, and (c) of $b$.

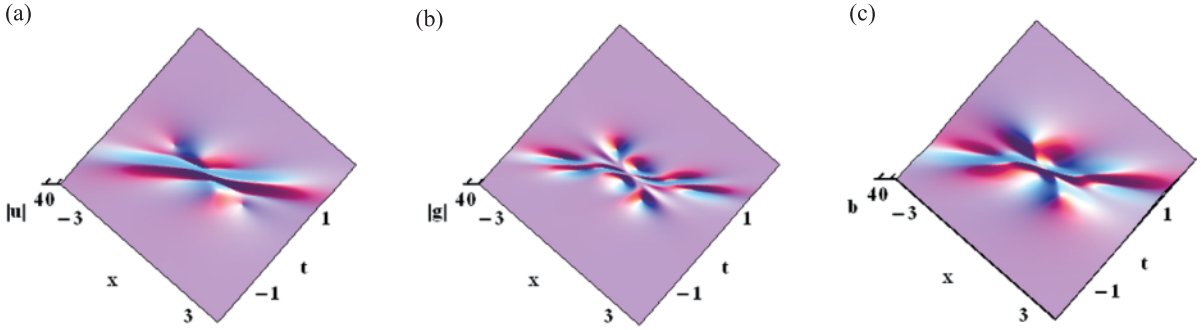


Fig. 9 (colour online). Second-order rogue-wave interaction as given by (32) with $a = \frac{1}{3}$ corresponding to (a) of $u$, (b) of $g$, and (c) of $b$.

of each soliton remain unchanged after the interaction.

(iii) Rogue-wave interaction and propagation have been analyzed:

Figures 4 and 5 have displayed that the coefficient $a$ has an effect on the distance of the first-order rogue-wave propagation: it is longer in Figure 5 than in Figure 4 when $a = 0$ in Figure 4 and $a = \frac{1}{3}$ in Figure 5.

Figures 5 and 6 have exhibited that the coefficient $a$ has an effect on the direction of the first-order rogue-wave propagation, i. e., Figure 5 has shown that it is consistent with the positive $x$-axis when $a = \frac{1}{3}$, and Figure 6 has displayed that it is consistent with the negative $x$-axis when $a = -\frac{1}{3}$.

Figures 7–9 have shown Second-Order Rogue-Wave Solutions (31) of (3). It has been found that the second-order rogue wave has the same properties as those of the first-order:

Coefficient $a$ has an effect on the range of the second-order rogue-wave interaction: the range in Figure 7a is larger than that in Figure 8a, the range in Figure 7b is larger than that in Figure 8b, and the range in Figure 7c is larger than that in Figure 8c when $a = 0$ in Figure 7 and $a = -\frac{1}{6}$ in Figure 8.

Coefficient $a$ has an effect on the direction of the second-order rogue-wave interaction: Figure 8 has shown that it is consistent with the negative $x$-axis when $a = -\frac{1}{6}$, and Figure 9 has displayed that it is consistent with the positive $x$-axis when $a = \frac{1}{3}$.

Moreover, Figures 4–9 have exhibited that $u$ is a bright rogue-wave, $g$ is a dark rogue-wave, and $b$ is a bright rogue-wave.

*Acknowledgements*

We express our sincere thanks to all the members of our discussion group for their valuable comments. This work has been supported by the State Key Laboratory of Software Development Environment (Grant No. SKLSDE-2014ZX-15), Beijing University of Aeronautics and Astronautics, by the Open Fund of State Key Laboratory of Information Photonics and Optical Communications (Beijing University of Posts and Telecommunications) under Grant No. IPOC2013B008, and by the National Natural Science Foundation of China under Grant No. 11272023.

## Appendix

$$
\begin{aligned}
\widehat{\widehat{u^{[2]}}} &= 45+432\mathrm{i}t-720t^2-18000a^2t^2+3072\mathrm{i}t^3-110592\mathrm{i}a^2t^3-11520t^4-13824a^2t^4-518400a^4t^4-12288\mathrm{i}t^5\\
&-221184\mathrm{i}a^2t^5-995328\mathrm{i}a^4t^5+4096t^6+110592a^2t^6+995328a^4t^6+2985984a^6t^6+5616atx+18432\mathrm{i}at^2x\\
&+23040at^3x+290304a^3t^3x+73728\mathrm{i}at^4x+663552\mathrm{i}a^3t^4x-36864at^5x-663552a^3t^5x-2985984a^5t^5x-180x^2\\
&-3456t^2x^2-58752a^2t^2x^2-6144\mathrm{i}t^3x^2-165888\mathrm{i}a^2t^3x^2+3072t^4x^2+165888a^2t^4x^2+1244160a^4t^4x^2+4992atx^3\\
&+18432\mathrm{i}at^2x^3-18432at^3x^3-276480a^3t^3x^3-144x^4-768\mathrm{i}tx^4+768t^2x^4+34560a^2t^2x^4-2304atx^5+64x^6,\\
\widehat{u^{[2]}} &= 9+432t^2+20016a^2t^2+3840t^4+152064a^2t^4-269568a^4t^4+4096t^6+110592a^2t^6+995328a^4t^6\\
&+2985984a^6t^6-2448atx-32256at^3x+124416a^3t^3x-36864at^5x-663552a^3t^5x-2985984a^5t^5x+108x^2\\
&+1152t^2x^2-17280a^2t^2x^2+3072t^4x^2+165888a^2t^4x^2+1244160a^4t^4x^2+384atx^3-18432at^3x^3-276480a^3t^3x^3\\
&+48x^4+768t^2x^4+34560a^2t^2x^4-2304atx^5+64x^6,\\
\widehat{\widehat{g^{[2]}}} &= 81+1296\mathrm{i}t-2592t^2+360288a^2t^2+48384\mathrm{i}t^3+6158592\mathrm{i}a^2t^3-186624t^4-38361600a^2t^4+395788032a^4t^4\\
&+663552\mathrm{i}t^5-29638656\mathrm{i}a^2t^5-320495616\mathrm{i}a^4t^5-3096576t^6-424230912a^2t^6-3443834880a^4t^6\\
&-10737598464a^6t^6+3538944\mathrm{i}t^7-548536320\mathrm{i}a^2t^7-8949989376\mathrm{i}a^4t^7+76536741888\mathrm{i}a^6t^7-19464192t^8\\
&-1290534912a^2t^8-13409058816a^4t^8-204671287296a^6t^8+192201818112a^8t^8-3145728\mathrm{i}t^9\\
&-2151677952\mathrm{i}a^2t^9-40259026944\mathrm{i}a^4t^9-210977685504\mathrm{i}a^6t^9-185752092672\mathrm{i}a^8t^9-44040192t^{10}\\
&-622854144a^2t^{10}+2378170368a^4t^{10}+45864714240a^6t^{10}-123834728448a^8t^{10}-1609851469824a^{10}t^{10}\\
&-50331648\mathrm{i}t^{11}-2264924160\mathrm{i}a^2t^{11}-40768634880\mathrm{i}a^4t^{11}-366917713920\mathrm{i}a^6t^{11}\\
&-1651129712640\mathrm{i}a^8t^{11}-2972033482752\mathrm{i}a^{10}t^{11}+16777216t^{12}+905969664a^2t^{12}+20384317440a^4t^{12}\\
&+244611809280a^6t^{12}+1651129712640a^8t^{12}+5944066965504a^{10}t^{12}+8916100448256a^{12}t^{12}-44064atx\\
&-393984\mathrm{i}at^2x-41472at^3x-95758848a^3t^3x-17252352\mathrm{i}at^4x-200392704\mathrm{i}a^3t^4x+76529664at^5x\\
&+1722580992a^3t^5x+6246678528a^5t^5x+3538944\mathrm{i}at^6x+1380188160\mathrm{i}a^3t^6x-60484091904\mathrm{i}a^5t^6x\\
&+379846656at^7x+10977804288a^3t^7x+167979515904a^5t^7x-201231433728a^7t^7x+415236096\mathrm{i}at^8x\\
&+21403533312\mathrm{i}a^3t^8x+186516504576\mathrm{i}a^5t^8x+247669456896\mathrm{i}a^7t^8x+358612992at^9x+2038431744a^3t^9x\\
&-21403533312a^5t^9x+165112971264a^7t^9x+2352859840512a^9t^9x+754974720\mathrm{i}at^{10}x+27179089920\mathrm{i}a^3t^{10}x\\
&+366917713920\mathrm{i}a^5t^{10}x+2201506283520\mathrm{i}a^7t^{10}x+4953389137920\mathrm{i}a^9t^{10}x-301989888at^{11}x\\
&-13589544960a^3t^{11}x-244611809280a^5t^{11}x-2201506283520a^7t^{11}x-9906778275840a^9t^{11}x\\
&-17832200896512a^{11}t^{11}x+1944x^2+5184\mathrm{i}tx^2+114048t^2x^2+10005120a^2t^2x^2+552960\mathrm{i}t^3x^2\\
&+68677632\mathrm{i}a^2t^3x^2+995328t^4x^2-223617024a^2t^4x^2-1336725504a^4t^4x^2+11501568\mathrm{i}t^5x^2+405209088\mathrm{i}a^2t^5x^2\\
&+19277512704\mathrm{i}a^4t^5x^2-25362432t^6x^2-2857697280a^2t^6x^2-56232050688a^4t^6x^2+89866174464a^6t^6x^2\\
&-9437184\mathrm{i}t^7x^2-3991928832\mathrm{i}a^2t^7x^2-67523051520\mathrm{i}a^4t^7x^2-144473849856\mathrm{i}a^6t^7x^2-42467328t^8x^2\\
&-1415577600a^2t^8x^2-1274019840a^4t^8x^2-96315899904a^6t^8x^2-1516975423488a^8t^8x^2-62914560\mathrm{i}t^9x^2\\
&-6794772480\mathrm{i}a^2t^9x^2-152882380800\mathrm{i}a^4t^9x^2-1284211998720\mathrm{i}a^6t^9x^2-3715041853440\mathrm{i}a^8t^9x^2\\
&+25165824t^{10}x^2+3397386240a^2t^{10}x^2+101921587200a^4t^{10}x^2+1284211998720a^6t^{10}x^2\\
&+7430083706880a^8t^{10}x^2+16346184155136a^{10}t^{10}x^2-521856atx^3-4976640\mathrm{i}at^2x^3+4202496at^3x^3\\
&+121872384a^3t^3x^3-84344832\mathrm{i}a^4x^3-3137273856\mathrm{i}a^3t^4x^3+286064640at^5x^3+9778102272a^3t^5x^3
\end{aligned}
$$

$$-22311272448a^5t^5x^3+292552704\mathrm{i}at^6x^3+12740198400\mathrm{i}a^3t^6x^3+48157949952\mathrm{i}a^5t^6x^3+257949696at^7x^3$$
$$+2548039680a^3t^7x^3+32105299968a^5t^7x^3+564135985152a^7t^7x^3+754974720\mathrm{i}at^8x^3+33973862400\mathrm{i}a^3t^8x^3$$
$$+428070666240\mathrm{i}a^5t^8x^3+1651129712640\mathrm{i}a^7t^8x^3-377487360at^9x^3-22649241600a^3t^9x^3$$
$$-428070666240a^5t^9x^3-3302259425280a^7t^9x^3-9081213419520a^9t^9x^3+12528x^4+96768\mathrm{i}tx^4+193536t^2x^4$$
$$-3068928a^2t^2x^4+3317760\mathrm{i}t^3x^4+270065664\mathrm{i}a^2t^3x^4-8773632t^4x^4-924991488a^2t^4x^4+3374161920a^4t^4x^4$$
$$-5898240\mathrm{i}t^5x^4-1309409280\mathrm{i}a^2t^5x^4-10032906240\mathrm{i}a^4t^5x^4-14942208t^6x^4-601620480a^2t^6x^4$$
$$-6688604160a^4t^6x^4-132434362368a^6t^6x^4-31457280\mathrm{i}t^7x^4-4246732800\mathrm{i}a^2t^7x^4-89181388800\mathrm{i}a^4t^7x^4$$
$$-481579499520\mathrm{i}a^6t^7x^4+15728640t^8x^4+2831155200a^2t^8x^4+89181388800a^4t^8x^4+963158999040a^6t^8x^4$$
$$+3405455032320a^8t^8x^4-193536atx^5-11280384\mathrm{i}at^2x^5+44679168at^3x^5-322486272a^3t^3x^5$$
$$+68419584\mathrm{i}at^4x^5+1337720832\mathrm{i}a^3t^4x^5+58982400at^5x^5+891813888a^3t^5x^5+20065812480a^5t^5x^5$$
$$+283115520\mathrm{i}at^6x^5+11890851840\mathrm{i}a^3t^6x^5+96315899904\mathrm{i}a^5t^6x^5-188743680at^7x^5-11890851840a^3t^7x^5$$
$$-192631799808a^5t^7x^5-908121341952a^7t^7x^5+11520x^6+165888\mathrm{i}tx^6-847872t^2x^6+19795968a^2t^2x^6$$
$$-1376256\mathrm{i}t^3x^6-111476736\mathrm{i}a^2t^3x^6-2162688t^4x^6-74317824a^2t^4x^6-1895104512a^4t^4x^6-7864320\mathrm{i}t^5x^6$$
$$-990904320\mathrm{i}a^2t^5x^6-13377208320\mathrm{i}a^4t^5x^6+5242880t^6x^6+990904320a^2t^6x^6+26754416640a^4t^6x^6$$
$$+176579149824a^6t^6x^6-774144atx^7+5308416\mathrm{i}at^2x^7+3538944at^3x^7+95551488a^3t^3x^7+47185920\mathrm{i}at^4x^7$$
$$+1274019840\mathrm{i}a^3t^4x^7-47185920at^5x^7-2548039680a^3t^5x^7-25225592832a^5t^5x^7+16128x^8-110592\mathrm{i}tx^8$$
$$-73728t^2x^8-663552a^2t^2x^8-983040\mathrm{i}t^3x^8-79626240\mathrm{i}a^2t^3x^8+983040t^4x^8+159252480a^2t^4x^8$$
$$+2627665920a^4t^4x^8-172032atx^9+2949120\mathrm{i}at^2x^9-5898240at^3x^9-194641920a^3t^3x^9+6144x^{10}$$
$$-49152\mathrm{i}tx^{10}+98304t^2x^{10}+9732096a^2t^2x^{10}-294912atx^{11}+4096x^{12},$$

$$\widehat{g^{[2]}}=\Big(9+432t^2+20016a^2t^2+3840t^4+152064a^2t^4-269568a^4t^4+4096t^6+110592a^2t^6+995328a^4t^6$$
$$+2985984a^6t^6-2448atx-32256at^3x+124416a^3t^3x-36864at^5x-663552a^3t^5x-2985984a^5t^5x+108x^2$$
$$+1152t^2x^2-17280a^2t^2x^2+3072t^4x^2+165888a^2t^4x^2+1244160a^4t^4x^2+384atx^3-18432at^3x^3-276480a^3t^3x^3$$
$$+48x^4+768t^2x^4+34560a^2t^2x^4-2304atx^5+64x^6\Big)^2,$$

$$\widehat{\widehat{b^{[2]}}}=384t\Big(-162at-2304at^3-1230336a^3t^3+64512at^5-6912000a^3t^5-57480192a^5t^5+393216at^7$$
$$-5308416a^3t^7+63700992a^5t^7+1289945088a^7t^7+393216at^9+14155776a^3t^9+191102976a^5t^9$$
$$+1146617856a^7t^9+2579890176a^9t^9+27x+1152t^2x+152064a^2t^2x+13824t^4x+1981440a^2t^4x$$
$$+29984256a^4t^4x+884736a^2t^6x-58392576a^4t^6x-1361608704a^6t^6x-65536t^8x-7077888a^2t^8x$$
$$-159252480a^4t^8x-1337720832a^6t^8x-3869835264a^8t^8x-3456atx^2-133632at^3x^2-5349888a^3t^3x^2$$
$$+147456at^5x^2+21233664a^3t^5x^2+609140736a^5t^5x^2+1179648at^7x^2+53084160a^3t^7x^2+668860416a^5t^7x^2$$
$$+2579890176a^7t^7x^2-768t^2x^3+338688a^2t^2x^3-24576t^4x^3-3833856a^2t^4x^3-149299200a^4t^4x^3-65536t^6x^3$$
$$-8847360a^2t^6x^3-185794560a^4t^6x^3-1003290624a^6t^6x^3-576atx^4+344064at^3x^4+21565440a^3t^3x^4$$
$$+737280at^5x^4+30965760a^3t^5x^4+250822656a^5t^5x^4-288x^5-12288t^2x^5-1824768a^2t^2x^5-24576t^4x^5$$
$$-3096576a^2t^4x^5-41803776a^4t^4x^5+82944atx^6+172032at^3x^6+4644864a^3t^3x^6-1536x^7-4096t^2x^7$$
$$-331776a^2t^2x^7+13824atx^8-256x^9\Big),$$

$$\widehat{b^{[2]}}=\Big(9+432t^2+20016a^2t^2+3840t^4+152064a^2t^4-269568a^4t^4+4096t^6+110592a^2t^6+995328a^4t^6$$

$$+2985984a^6t^6-2448atx-32256at^3x+124416a^3t^3x-36864at^5x-663552a^3t^5x-2985984a^5t^5x+108x^2$$
$$+1152t^2x^2-17280a^2t^2x^2+3072t^4x^2+165888a^2t^4x^2+1244160a^4t^4x^2+384atx^3-18432at^3x^3-276480a^3t^3x^3$$
$$+48x^4+768t^2x^4+34560a^2t^2x^4-2304atx^5+64x^6\Big)^2.$$


[1] W. R. Sun, B. Tian, Y. Jiang, and H. L. Zhen, Ann. Phys. **343**, 215 (2014).
[2] M. J. Ablowitz and P. A. Clarkson, Solitons, Nonlinear Evolution Equations and Inverse Scattering, Cambridge Univ. Press, Cambridge 1991.
[3] X. F. Pang, Soliton Physics, Sichuan Sci.-Tech. Press, Chengdu 2003.
[4] W. R. Sun, B. Tian, H. Zhong, and H. L. Zhen, Stud. Appl. Math **132**, 65 (2014).
[5] R. Hirota, The Direct Method in Soliton Theory, Cambridge Univ. Press, Cambridge 2004.
[6] B. L. Guo, L. M. Ling, and Q. P. Liu, Phys. Rev. E **85**, 26607 (2012).
[7] D. R. Solli, C. Ropers, P. Koonath, and B. Jalali, Nature **405**, 1054 (2007).
[8] G. P. Agrawal, Nonlinear Fiber Optics, Academic, New York 1995.
[9] F. Smirnov, Form Factors in Completely Integrable Models of Quantum Field Theory, World Sci., Singapore 1992.
[10] P. K. Shukla and B. Eliasson, Phys. Usp. **53**, 51 (2010).
[11] A. Hesegawa and Y. Kodama, Solitons in Optical Communication, Oxford Univ. Press, Oxford 1995.
[12] A. Ankiewicz, J. M. Soto-Crespo, and N. Akhmediev, Phys. Rev. E **81**, 46602 (2010).
[13] N. Akhmediev, V. M. Eleonskii, and N. E. Kulagin, Theor. Math. Phys. **72**, 809 (1987).
[14] N. Akhmediev, A. Ankiewicz, and J. M. Soto-Crespo, Phys. Rev. E **80**, 26601 (2009).
[15] A. Chabchoub, N. P. Hoffmann, and N. Akhmediev, Phys. Rev. Lett. **106**, 204502 (2011).
[16] N. Benes, A. Kasman, and K. Young, J. Nonlin. Sci. **16**, 179 (2006).
[17] I. Christov and C. I. Christov, Phys. Lett. A **372**, 841 (2008).
[18] Y. Jiang, B. Tian, M. Li, and P. Wang, Nonlin. Dyn. **74**, 1053 (2013).
[19] Yu. V. Sedletsky, J. Exp. Theor. Phys. **97**, 180 (2003).
[20] Y. Jiang and B. Tian, Europhys. Lett. **102**, 10010 (2013).
[21] A. V. Slunyaev, J. Exp. Theor. Phys. **101**, 926 (2005).
[22] W. Ames, Nonlinear partial differential equations, Academic Press, New York 1967.
[23] R. Sahadevan and L. Nalinidevi, J. Nonlin. Math. Phys. **17**, 517 (2010).
[24] R. Sahadevan and L. Nalinidevi, J. Nonlin. Math. Phys. **17**, 379 (2010).
[25] C. Z. Li, S. J. He, and K. Porsezian, Phys. Rev. E **87**, 12913 (2013).
[26] K. Porsezian and K. Nakkeeran, Phys. Rev. Lett. **74**, 2941 (1995).
[27] B. Tian and Y. T. Gao, Phys. Lett. A **340**, 243 (2005).
[28] T. Xu, B. Tian, L. L. Li, X. Lü, and C. Zhang, Phys. Plasmas **15**, 102307 (2008).
[29] Y. Zhang, Y. Song, L. Cheng, J. Y. Ge, and W. W. Wei, Nonlin. Dyn. **68**, 445 (2012).
[30] M. J. Ablowitz, D. J. Kaup, A. C. Newell, and H. Segur, Phys. Rev. Lett. **31**, 125 (1973).
[31] C. W. Cao, Sci. Chin. A **33**, 528 (1990).
[32] H. L. Zhen, B. Tian, and W. R. Sun, Appl. Math Lett. **27**, 90 (2014).
[33] G. Neugebauer and R. Meinel, Phys. Lett. A **100**, 467 (1984).
[34] C. H. Gu, H. S. Hu, and Z. X. Zhou, Darboux Transformation in Integrable Systems: Theory and their Applications to Geometry, Springer, Dordrecht 2005.
[35] V. B. Matveev, Phys. Lett. A **166**, 205 (1992).
[36] H. L. Zhen, B. Tian, Y. F. Wang, H. Zhong, and W. R. Sun, Phys. Plasmas **21**, 12304 (2014).
[37] D. W. Zuo, Y. T. Gao, Y. J. Feng, and L. Xue, Nonlin. Dyn., in press, doi:10.1007/s11071-014-1557-0 (2014).
[38] L. C. Zhao and J. Liu, J. Opt. Soc. Am. B **29**, 3119 (2012).